

1 **Integrated distribution modelling to estimate the national population size of**  
2 **an alpine bird**

3

4 Diana E. Bowler<sup>1-3\*</sup>, Erlend B. Nilsen<sup>4,5</sup>

5

6 1. German Centre for Integrative Biodiversity Research (iDiv), Deutscher Platz 5E, 04103

7 Leipzig, Germany

8 2. Institute of Biodiversity, Friedrich Schiller University Jena, Dornburger Straße 159, 07743

9 Jena, Germany

10 3. Helmholtz Center for Environmental Research - UFZ, Department of Ecosystem Services,

11 Permoserstraße 15, 04318 Leipzig, Germany

12 4. Norwegian Institute for Nature Research, P.O. 5685 Torgarden, 7485 Trondheim, Norway

13 5. Nord University, Universitetsalléen 11, 8026 Bodø, Norway

14

15 \* Corresponding author: [diana.e.bowler@gmail.com](mailto:diana.e.bowler@gmail.com)

16

17 **Abstract:**

- 18 1) Estimates of species' population abundances have important ramifications for  
19 conservation decision-making. Conservation practice, however, often has to rely on  
20 indices of relative abundance rather than absolute estimates. Attempts to estimate  
21 large-scale abundance estimates of species are limited by both the availability of data  
22 and statistical challenges. New opportunities are, however, emerging as a result of the  
23 development of an open data culture.
- 24 2) Here we integrate information from two distinct citizen science data sources,  
25 opportunistic occurrence data and targeted standardized distance-sampling survey  
26 data, to estimate the population size of an alpine bird - the willow ptarmigan, *Lagopus*  
27 *lagopus* - in Norway between 2008 and 2017. Our model combines the strengths of the  
28 occurrence data (widespread but coarse) and standardised survey data (spatially  
29 restricted but detailed) to estimate ptarmigan population size at both local and  
30 national-scales. Using simulations, we also examined the sensitivity of the population  
31 size estimates to each data type to guide future data collection.
- 32 3) An occupancy-detection model fit to the occurrence data predicted that willow  
33 ptarmigan were present in 29% of 5 x 5 grid cells across Norway. Occupancy  
34 probability was most strongly affected by habitat covariates. The distance-sampling  
35 model predicted that ptarmigan density in the area covered by the line-transect surveys  
36 was, on average, 13 individuals per km<sup>2</sup>, and most strongly affected by climatic  
37 variables. On integration, we predicted a mean annual population size of c. 1.2 million  
38 individuals.
- 39 4) Most of the uncertainty in the national population size estimate was driven by  
40 uncertainty in occupancy in western and central Norway. Hence, data collection

41 activities might be encouraging in these regions to increase the precision of population  
42 size estimate.

43 5) *Synthesis and applications*: Our study shows the possibilities of new data sources and  
44 modelling approaches to provide absolute estimates of species' population sizes,  
45 which are often more revealing than relative abundance indices for understanding  
46 species' population dynamics and trends. Ecologists can take advantage of the open  
47 data revolution, and especially the relative strengths of different available data types,  
48 to estimate species' abundance at large spatial scales.

49

50 Keywords: citizen science; data integration; integrated distribution models; population  
51 abundance; population size; species monitoring; synthesis

## 52 Introduction

53 Species' abundance plays a central role in most ecological and evolutionary processes  
54 (Kunin 1998; McGill & Collins 2003). Monitoring programs typically collect abundance data  
55 to create indices of the relative abundance of species (Van Strien, Pannekoek & Gibbons  
56 2001; Collen *et al.* 2009), which are sufficient for many questions about trends (Dornelas *et*  
57 *al.* 2019) and drivers of trends (Kolecek *et al.* 2014). However, estimates of species' total or  
58 absolute abundances are also important, such as to inform the IUCN red list assessment  
59 (IUCN 2012), for reference levels to define conservation targets (Reed *et al.* 2003), or to  
60 assign sustainable harvest quotas (Eriksen, Moa & Nilsen 2018). However, few monitoring  
61 schemes aim to go beyond abundance indices to estimate the total number of individuals  
62 within a population, especially at large spatial scales. With the current reliance on abundance  
63 indices, there is a risk that the value of absolute population abundance estimates is overlooked  
64 for understanding species' population dynamics and trends.

65 The main challenge to the quantification of species abundances at large spatial scales  
66 is imperfect detection and spatial heterogeneity in abundance (Yoccoz, Nichols & Boulinier  
67 2001; Jones 2011). Imperfect detection arises because some individuals are almost always  
68 missed during a survey within a target area (Kéry & Royle 2016). Abundance models that  
69 ignore imperfect detection make the simplistic assumption that species' detection probabilities  
70 are constant among different places and at different times (i.e. similar fractions of individuals  
71 are missed during a survey) (Pollock *et al.* 2002; Johnson 2008). By contrast, models that  
72 account for imperfect detection allow for variation in species' detectability and can therefore  
73 provide better information on spatial and temporal patterns in species abundance (Pollock *et*  
74 *al.* 2002; Hewson *et al.* 2018). Species' detection probabilities, and in turn total abundance  
75 estimates, can be estimated using methods for marked (i.e., tagged) individuals, e.g., mark-  
76 recapture (McCrea & Morgan 2014), or for unmarked individuals, such as distance-sampling

77 methods (Buckland *et al.* 2001) or repeat surveys (Botsch, Jenni & Kery 2020). However,  
78 these methods are costly in terms of sampling frequency or effort, which means that they tend  
79 to be only possible at a small spatial scale for local abundance estimates. Estimating  
80 abundance at large spatial scales remains a challenge due to spatial variation in abundance,  
81 which means that surveyed areas might be a poor representation of the wider landscape  
82 (Buckland & Johnston 2017). This is especially true when the survey was focused on the core  
83 habitat of a species.

84         Upscaling of abundance estimates from local-scale abundance data may be possible by  
85 combining it with other data types that provide coarser but more widespread information on  
86 species' populations (Pagel *et al.* 2014; Isaac *et al.* 2020; Farr *et al.* 2021). Opportunistic  
87 occurrence data that have been collected without a common survey protocol, typically from  
88 citizen scientists, can potentially provide data over a large spatial scale, including from both  
89 core and marginal areas for a species (Kery, Gardner & Monnerat 2010; Soroye, Ahmed &  
90 Kerr 2018). In the last decade, hierarchical models have been developed that deal with the  
91 inherent biases within such opportunistic citizen science data (van Strien, van Swaay &  
92 Termaat 2013; Isaac *et al.* 2014). Moreover, recent studies have also shown how different  
93 types of data, including abundance and occurrence, can be combined together to increase the  
94 sample size and spatial coverage (Miller *et al.* 2019; Isaac *et al.* 2020).

95         Here, we show how occurrence data and abundance data can be combined by using  
96 integrated modelling to estimate total abundance for an iconic alpine species. More precisely,  
97 we estimate the national population size of the willow ptarmigan *Lagopus lagopus* in Norway.  
98 This species is thought to have already undergone a large decline in the 20<sup>th</sup> century  
99 (Lehikoinen *et al.* 2019). Moreover, as an alpine species, it is especially vulnerable to on-  
100 going and future climate change (Bowler *et al.* 2020). We combined information on density,  
101 from distance-sampled line-transect surveys that targeted the core alpine habitat of the

102 ptarmigan, with occurrence data that provided information on the larger distribution of bird  
103 species across Norway. Moreover, we examined the uncertainty of the model to identify  
104 which geographic regions might be further sampled to improve the national population size  
105 estimate.

## 106 Materials and methods

### 107 Occurrence data

108 Occurrence data for Norway were downloaded from GBIF and the Species map service of the  
109 Norwegian Biodiversity Information Centre. Data are collected by variable methods and are  
110 best regarded as opportunistic i.e., without a consistent sampling protocol. We downloaded  
111 two sets of data: (1) occurrence data for willow ptarmigan and (2) occurrence data for all  
112 birds (Fig. 1). Data for all bird occurrences were used in the statistical analysis to control for  
113 spatial and temporal variation in the sampling effort of ornithologists across Norway. The  
114 willow ptarmigan occurrence dataset included some observations from the line-transect  
115 surveys; however, we did not discard them from the occurrence data set since they still  
116 provided valid occurrence observations. Both sets of data were filtered by removing: duplicate  
117 observations (with the same date, species and geographic coordinates); those with coordinate  
118 uncertainty greater than 5 km; those with geographic coordinates with less than three decimal  
119 places and those outside our temporal scope of 2008-2017. We focused on records during the  
120 breeding season between May and September. The occurrence data were mapped to a  
121 reference grid comprising 5 x 5 km grid cells that covered the extent of Norway (limited to  
122 grids that overlapped at least 50% with mainland Norway). This resolution should account for  
123 limited local movement of the ptarmigan within the summer season and aligned with the  
124 mean length of the line-transect surveys (see next section).

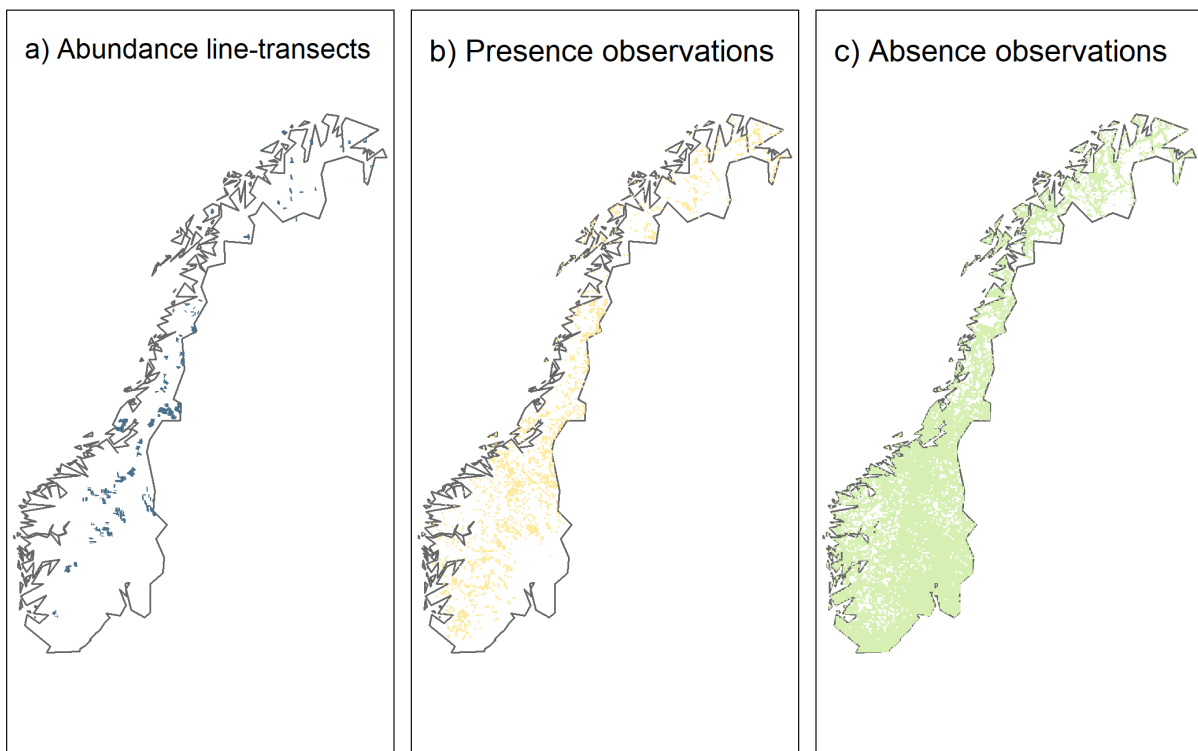
125

### 126 Line-transect survey data

127 We used a dataset of line-transect surveys that covered almost the full latitudinal extent of  
128 mainland Norway for 2008–2017 (Fig. 1). The surveys come from a structured citizen science  
129 program that is coordinated by local and regional initiatives. The program targeted the willow

130 ptarmigan and focused on its core habitat in alpine areas. Volunteer surveyors follow a  
131 common survey procedure using distance-sampling methods, usually in August (Nilsen *et al.*  
132 2020). See Bowler *et al.* (2020) for more details. We excluded observations made at distances  
133 greater than 200 m from the transect line, as well as detections by the surveyor, and not by the  
134 trained pointing dogs, at distances > 10 m away from the transect line. We used data from 585  
135 line-transects (mean length of 4.3 km) that were visited in at least 5 years (a median of 10  
136 years) during our study period.

137



138

139 Fig. 1 Maps showing the distributions of each data set: (a) line-transect surveys from  
140 structured citizen science that targeted the willow ptarmigan and (b) presence and (c) absence  
141 observations for the willow ptarmigan (i.e. bird species were reported on a given date and  
142 place but not the willow ptarmigan) from opportunistic citizen science.

143



144 Environmental covariates

145 *Climate:* We used the EuroLST dataset that provides summary temperature maps derived  
146 from reconstructed MODIS LST averaged for 2001–2013 at 250 m resolution (Metz,  
147 Rocchini & Neteler 2014). We used data on maximum temperature of the warmest month and  
148 minimum temperature of the coldest month.

149 *Habitat:* We used a vegetation map of Norway, which used satellite data to classify land cover  
150 at 30 m resolution into 25 classes (Johansen, Aarrestad et al. 2009). The land classes were  
151 aggregated into percentage cover of: mountain birch forest; boreal/lowland forest; bogs with  
152 dense field layer; swamps/bogs with sparse field layer; open areas with dense field layer; open  
153 areas with sparse field layer and snowbeds, following Kvasnes et al. (2018) (Table S1).

154 *Treeline:* Elevation was extracted from a digital elevation model of Fennoscandia at 10 m  
155 resolution (<https://kartkatalog.geonorge.no/>). Treeline data at 100 m resolution was extracted  
156 from Blumenrath & Hanssen (2010). We calculated the deviation of the elevation from the  
157 predicted treeline for each grid cell.

158 *Region:* We obtained spatial polygon data on the administrative regions that subdivide  
159 Norway (<https://gadm.org/>, level 2).

160 Covariate data were matched to the occurrence data by averaging values within the 5 x 5 km  
161 grid cells and to the abundance data by averaging within circles (with areas of 25 km<sup>2</sup> to  
162 match the area of the grid cells) centred on the centroids of each line-transect.

163

164

165

166

167 Statistical analysis

168

169 Selection of environmental variables

170 We included both linear and quadratic effects of all continuous covariates in the models  
171 described below. We used variable indicator selection by multiplying the Gaussian prior on  
172 each covariate with a Bernoulli indicator variable that modified whether the variable was  
173 included in the model or not (Rushing *et al.* 2019). Alternative approaches were considered  
174 but they gave similar results (see SI).

175

176 Occurrence data

177 To estimate the probability of occurrence of willow ptarmigan, we first constructed a  
178 detection history for each 5 x 5 km grid cell. The spatial and temporal unit of our analysis was  
179 a visit, defined by a list of species observations collected on a given date in a given grid cell.  
180 For each visit, we created a binary indicator to reflect whether willow ptarmigan was included  
181 among the reported bird species (1=yes, 0=no). Hence, following others (van Strien, van  
182 Swaay & Termaat 2013), absence data (non-detections) for ptarmigan were inferred from  
183 observations of other bird species on a given visit. We used occupancy-detection models to  
184 analyse the detection/non-detection of species on a visit, which have been used in previous  
185 studies using similar heterogeneous data (Kery, Gardner & Monnerat 2010; Outhwaite *et al.*  
186 2020) and tested in simulation studies (Isaac *et al.* 2014). In occupancy-detections models, the  
187 detection probability of a species is estimated by the number of times a species was/was not  
188 reported during repeat visits to the same grid. We assumed closure (i.e. period of no change in  
189 occupancy during repeat visits) between April and October of each year.

190 Letting  $z_{i,t}$  refer to the true occupancy status for a species in grid  $i$  in year  $t$ , we  
 191 modelled occupancy probability ( $\psi$ ) as a function of fixed effects of the environmental  
 192 covariates and a series of random effects to account for clustering of the data in space and  
 193 time (spatial: administrative region and grid cell; temporal: year).

194 Hence, our occupancy model was:

$$z_{i,t} \sim \text{Bernoulli}(\psi_{i,t})$$

$$\text{logit}(\psi_{i,t}) = \beta_0 + \beta_e \text{ EnvironVars}_i + \text{Grid}_i + \text{Region}_i + \text{Year}_t$$

195  
 196  
 197  
 198 Detection probability ( $p$ ) was modelled for each visit  $j$  to a given grid in a given year,  
 199 and allowed to vary with variables expected to be most associated with species visibility and  
 200 abundance (open habitat cover, temperature and tree line). Following Outhwaite (2020),  
 201 survey effort was modelled as a function of list length, i.e., number of species reported on a  
 202 visit (a categorical variable – a single species, a short list (2-4 species), or a longer list – set as  
 203 the reference level). Random effects for year and region were also included.

$$\text{logit}(p_{i,t,j}) = \beta_0 + \beta_{det} \text{ EnvironVars}_i + \beta_{si} \text{ single\_list}_j + \beta_{sh} \text{ short\_list}_j + \text{Year}_t$$

$$+ \text{Region}_i$$

204  
 205  
 206  
 207 The observed detection data for the willow ptarmigan,  $y$  (0 for non-detection or 1 for  
 208 detection) on each visit are then assumed to be drawn from a Bernoulli distribution  
 209 conditional on the presence of the species in that grid cell and year:

$$y_{i,t,j} | z_{i,t} \sim \text{Bernoulli}(z_{i,t} \cdot p_{i,t,j})$$

210  
 211  
 212 The models were run in JAGS with 20,000 iterations and 10,000 burnin, with vague priors.  
 213 The Rhat statistics and traceplots were used to check for convergence.

214

215 Line-transect survey data

216 We fitted a distance-sampling detection model to estimate the effective strip width of each  
217 transect (Buckland *et al.* 2001). We modelled the perpendicular distances of ptarmigan  
218 observations from the transect line as a half-normal distribution, following an earlier study  
219 (Bowler *et al.* 2020). On the transect line, we assumed perfect detection – a common  
220 assumption in distance-sampling (Buckland *et al.* 2001). We modelled sigma - the parameter  
221 of the half-normal distribution that reflects the rate of distance-decay of detections - to be  
222 dependent on group size (i.e. the number of birds in each observation). To account for any  
223 spatial autocorrelation in sigma, we also included a random effect for region.

$$224 \quad \log(\sigma_{i,t}) = \beta_0 + \beta_{GS} \text{GroupSize}_{i,t} + \text{Region}_i$$

225

226 The effective strip width of each transect ( $i$ ) in each year ( $t$ ) was calculated from sigma  
227 by (Buckland *et al.* 2001):

$$228 \quad ESW_{i,t} = \sqrt{\frac{(\pi * \sigma_{i,t}^2)}{2}}$$

229

230 We then used the estimated effective strip width (ESW) and transect length (TL) to  
231 relate the total number of individuals observed along each transect,  $N$ , to the latent variable,  
232 ptarmigan density,  $D$ , (abundance per km<sup>2</sup>) for each transect  $i$  in year  $t$  :

$$233 \quad \text{Ptarmigan\_Obs}_{i,t} \sim \text{Negative Binomial}(N_{i,t}, r)$$

$$234 \quad N_{i,t} = D_{i,t} \times TL_{i,t} \times ESW_{i,t} \times 2$$

235 We assumed that the number of individuals,  $N_{i,t}$  followed a negative binomial distribution  
236 with constant dispersion parameter  $r$ . Like for occupancy, density was modelled as a function

237 of fixed effects of the environmental covariates and random effects to account for clustering  
238 of the data in space and time (spatial: administrative region and grid cell; temporal: year).

$$239 \quad \ln D_{i,t} = \beta_0 + \beta_e \text{ EnvironVars}_i + \text{Grid}_i + \text{Region}_i + \text{Year}_t$$

240 To spatially align the line-transect density predictions with the grid-level occupancy  
241 predictions, each line-transect was associated with the 5 x 5 km grid cell that overlapped with  
242 the line-transect centroid coordinates. The density per km estimated for each line-transect was  
243 then scaled to the associated 5 x 5 km grid by multiplying by 25, on the assumption that the  
244 line-transect was a representative sample of the grid. The models were run in JAGS with  
245 50,000 iterations and 25,000 burnin, with vague priors. The Rhat statistics and traceplots were  
246 used to check for convergence.

247

#### 248 Data integration

249 We followed the principle of a zero-inflated model to predict species abundance per 5 x 5 km  
250 grid cell over the whole extent of mainland Norway. A zero-inflated model assumes that  
251 species abundance is generated by two processes: one governing whether a grid is suitable for  
252 occupation and a second process governing the abundance of the species at suitable grids. We  
253 used the aforementioned occupancy-detection model for the first process and the distance-  
254 sampling model for the second process. Previous attempts to data integration have often used  
255 a joint-likelihood approach, which means that the ecological models were assumed as the  
256 same in each dataset (Miller et al. 2019). However, there is debate about whether occurrence  
257 and abundance are really outcomes of the same point processes governing the distribution of  
258 individuals (Kéry & Royle 2016). In our case, we felt justified in modelling each dataset  
259 separately based on the large differences in spatial extent between the two datasets and  
260 geographic space – the line-transects specifically targeting the alpine habitat of the ptarmigan.

261 Moreover, our datasets were not entirely independent (some of the presence observations  
262 came from the line-transect surveys) and a joint-likelihood approach could have over-  
263 estimated the precision in the estimated abundance.

264 We integrated the information in each dataset via multiplication of samples from the  
265 posterior distribution of grid-level predictions from the occupancy model and the distance-  
266 sampling model for each year. These models were used to make predictions of realized  
267 abundance to all grids across Norway, as follows:

$$268 \quad \textit{Realized abundance}_{i,t} = \textit{PredictedAbund}_{i,t} \times \textit{Pr(Occupancy)}_{i,t}$$

269  
270 To estimate the national population size, we summed the predictions across all grid  
271 cells. For comparison, we used a simpler approach, similar to the approach used by BirdLife  
272 International, which estimates total population abundance by multiplication of the estimated  
273 area of occupancy with estimated mean density. In our case, area of occupancy was based on  
274 the number of occupied grid cells predicted by the occupancy model (i.e. sum of the z across  
275 all grid cells) while mean density was the mean density predicted across all line-transects.

276

277 Model validation and predictive performance

278 *Within-sample:* We carried our posterior predictive checks by calculating a Bayesian p-value.  
279 Bayesian p-values close to 0 or 1 would indicate poor model fit (Kéry & Royle 2016). For the  
280 line-transect model, this was based on a Pearson chi-square statistics for the observed number  
281 of birds and for simulated values from the fitted model in comparison with the expectation of  
282 the linear predictor of the model. The p-value is then how often the discrepancy for the  
283 observed data is larger (or smaller) than the discrepancy for the simulated data. For the  
284 occupancy model, the Pearson chi-square statistic was calculated for the total number of birds

285 detected each year and for the simulated values from the fitted model, in comparison with the  
286 expected number from the fitted values (Tobler *et al.* 2015; Broms, Hooten & Fitzpatrick  
287 2016). We also used area under the curve (AUC) to quantify the discrimination of the  
288 occupancy model (Zipkin, Grant & Fagan 2012) and mean absolute deviation (MAD, average  
289 deviation between observation and predictions) for the line-transect model.

290 *Out-of-sample:* The latitudinal range of the data was split into 25 blocks that were  
291 systematically assigned to one of five folds (Fig. S1). We repeated the models described  
292 above five times - training using four of the folds (e.g., folds 1-4) and using the remaining  
293 fold (e.g., fold 5) for testing. For each fold we calculated the AUC to quantify the  
294 discrimination of the occupancy model (Zipkin, Grant & Fagan 2012), and MAD for the line-  
295 transect model. These statistics were calculated for the middle year of the time-series.  
296 Random site and region effects were not included in the models for cross-validation since the  
297 levels within the training dataset were not always within the test dataset.

298

#### 299 Uncertainty analysis

300 We used Monte Carlo simulation to examine how uncertainty in the grid-level predictions of  
301 occupancy and abundance led to uncertainty in the national population size estimates. We  
302 compared the effects of uncertainty of predictions for each grid and each data type by  
303 propagating uncertainty through for each grid and data type while holding constant the values  
304 for the remaining grids and data type. Specifically, uncertainty was examined by taking all  
305 grid values (except for one focal grid) for occupancy probability and abundance to be the  
306 mean of the posterior from the fitted model (i.e., the best estimate) but randomly sampling  
307 occupancy or abundance values from their posterior distributions for the remaining focal grid.  
308 For each random sample, a new total population size was arrived at calculating the realised

309 abundance (occupancy x abundance) of each grid and then summing the values across all  
310 grids. Random sampling was repeated 1000 times and the standard deviation of the total  
311 population sizes was calculated across the replicates.

312

313 All analyses were performed in R 4.1.0.

314

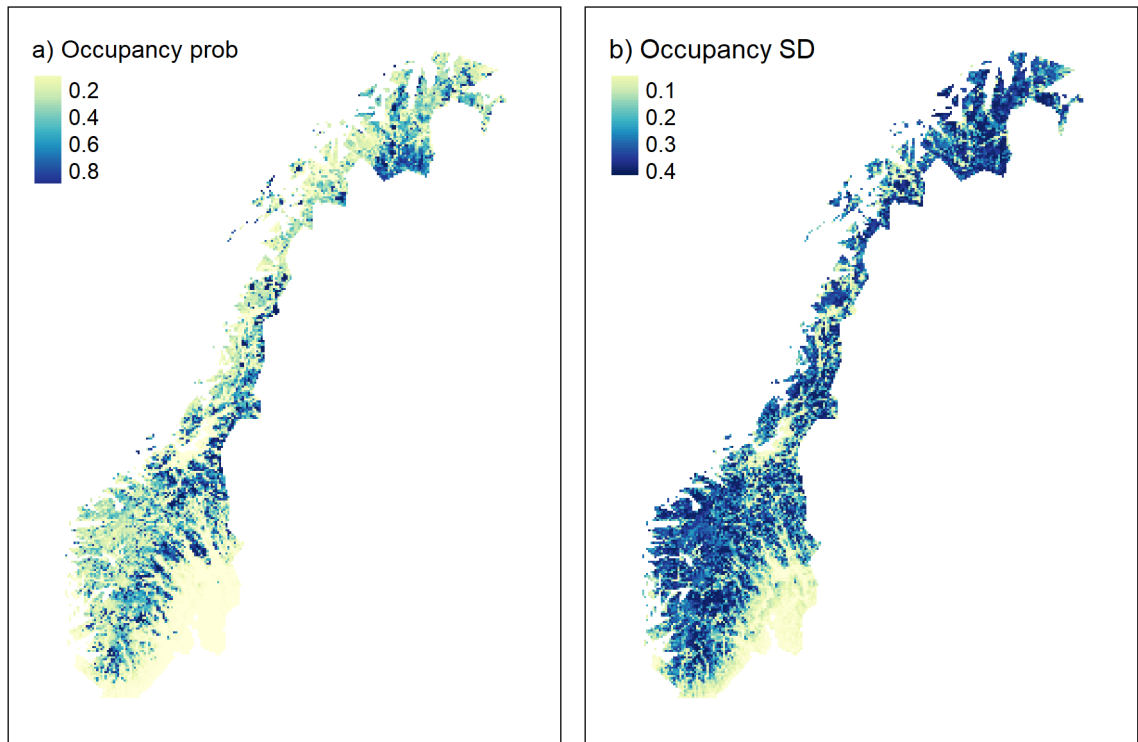


## 315 Results

### 316 Occupancy

317 Observations of at least one bird species were reported in 75.7% (n = 8927) of the 5 x 5 km  
318 grids that covered mainland Norway. In the study period, willow ptarmigan were reported at  
319 least once in 21.3 % (n=1898) of the sampled grids. Mean detection probability (i.e.  
320 probability to detect a ptarmigan if it is present within a grid) was 0.16 (95% CI = 0.14, 0.18).  
321 Detection probability was lower on visits reporting single (95% CI = -0.64, -0.49) or short  
322 species lists (95% CI = -1.08, -0.91), and greater in areas with more open habitat (95% CI =  
323 0.47, 0.57), colder temperatures (95% CI = 0.29, 0.45) and higher tree lines (95% CI = 1.20,  
324 1.73).

325 Mean occupancy probability across all grid cells was 0.29, but there was substantial  
326 spatial variation (Fig. 2). Occupancy probability was most positively affected by tree line  
327 (quadratic effect, with lower density at the highest tree lines), open dense vegetation, bog  
328 cover, mountain birch forest and temperature (Fig. S2). The Bayesian p-value was 0.47,  
329 suggesting no fit issues. AUCs were high (occupancy model median AUC = 0.97; detection  
330 model median AUC = 0.96). Cross validation showed that the detection model was weaker  
331 than the occupancy model, but AUCs on the test dataset were still reasonably good (Table  
332 S2).



333

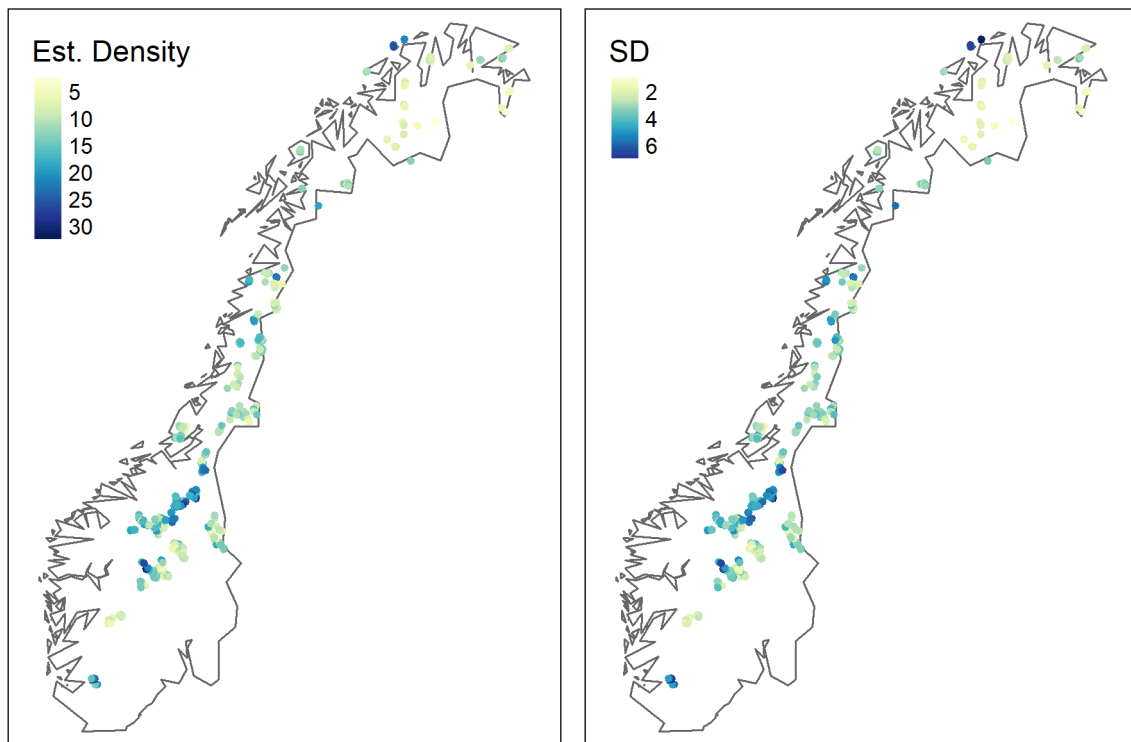
334 Fig. 2 Occupancy probability estimates of willow ptarmigan across Norway (a) and standard  
 335 deviation of the estimate (b) from the occupancy-detection model. Each pixel is a 5 x 5 km  
 336 grid.

337

### 338 Density

339 The 585 line-transects were placed within 302 (2.6 %) of the 5 x 5 km grids. Along each  
 340 transect, a median of six ptarmigan (interquartile range = 3–11) were observed each year. The  
 341 average effective strip width of the line-transects was 100 m (interquartile range = 90–110 m)  
 342 and was positively affected by ptarmigan group size (95% CI of coefficient on sigma = 0.37,  
 343 0.40), i.e., larger groups had higher detection probability at greater distances. Mean density of  
 344 willow ptarmigan per km<sup>2</sup> was estimated as 13 (interquartile range = 9–16) across all line-  
 345 transects (Fig. 3). Variable indicator selection supported the importance of variables related to  
 346 temperature (maximum and minimum temperature) and tree line (Fig. S3). For fit measures,

347 the model predictions were strongly correlated with the observed data ( $r = 0.93$ ; Fig S4); the  
348 mean absolute deviation was 2.39 (for the line-transect mean count) or 4.9 (for year-specific  
349 transect predicted count), and the Bayesian p-value was 0.58, suggesting no fit problems.  
350 Also, cross-validation suggested no great loss of fit between the test versus training datasets  
351 (Table S2).



352  
353 Fig. 3 Ptarmigan density estimates (abundance per km<sup>2</sup>) (left) and standard deviation of the  
354 estimate (right) from the distance-sample model of the line-transect survey data. Each dot  
355 reflects the location of a line-transect.

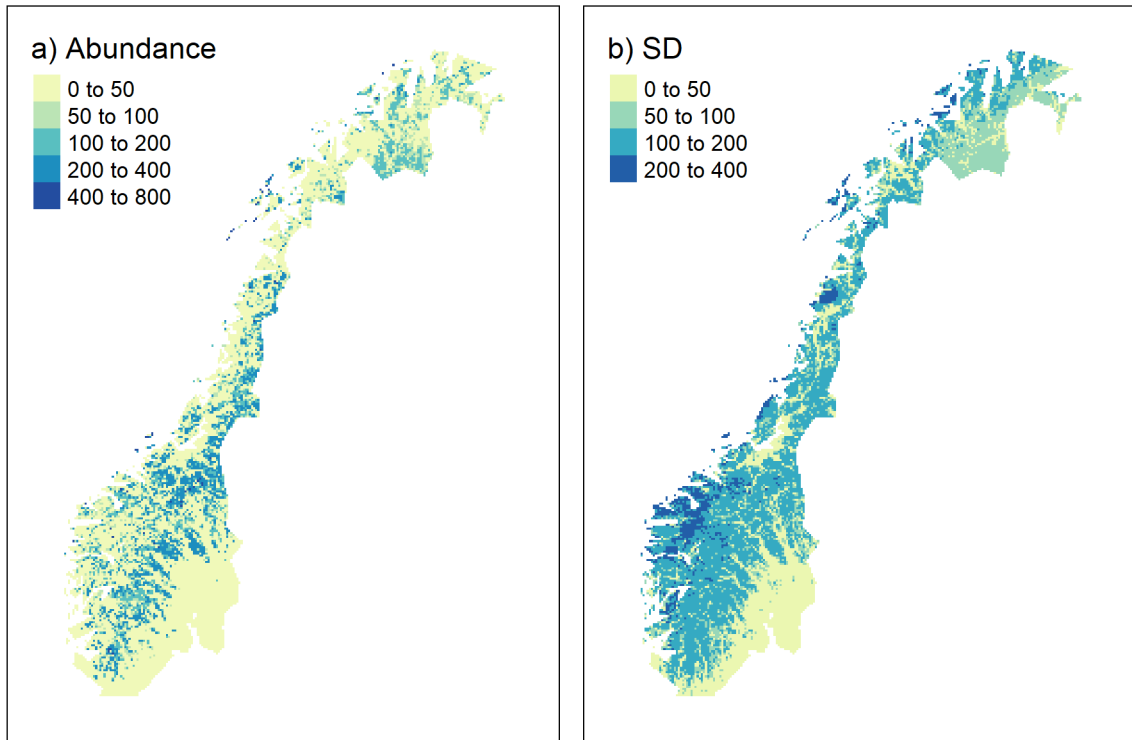
356

### 357 Data integration and total population size

358 Abundance was highest in central Norway and lowest in the southeast and north (Fig. 4).

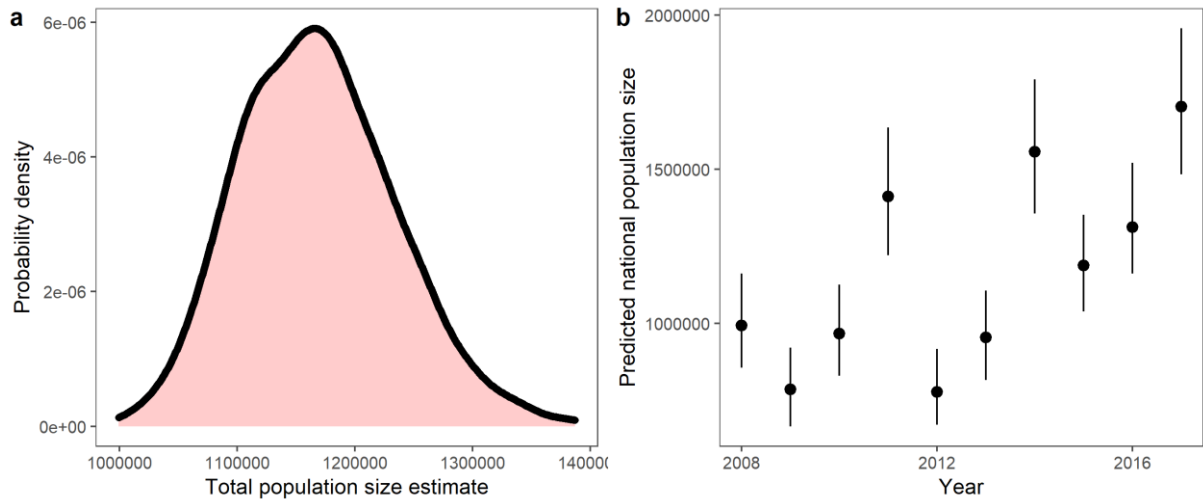
359 Summed across all grids, total abundance, on average across years, was 1,164,379 (95% CI =  
360 1,053,149 to 1,307,195) (Fig. 5a). This estimate was generally similar for all three approaches  
361 taken to select the environmental variables for the most parsimonious model (Fig. S5). Year-

362 specific predictions varied between 778,310 and 1,703,192 individuals, on average (Fig. 5b;  
363 see Bowler et al. 2020 for discussion on the drivers of cyclic dynamics). The simpler model to  
364 estimate total abundance (i.e., predicted number of occupied grids x mean density) led to a  
365 similar prediction of the total population size: 1,207,997.  
366



367  
368 Fig. 4 Integrated model predictions of abundance within each 5 x 5 km grid (left) and its  
369 standard deviation (right). The predictions combine information from both the line-transect  
370 surveys and the occurrence observations.

371



372

373 Fig. 5 (a) Posterior distribution of the estimated national population size of willow ptarmigan.  
 374 (b) Annual predictions of the population size; points are lines show means and 95% credible  
 375 intervals (see Bowler et al. 2020 for analysis of the cyclic dynamics).

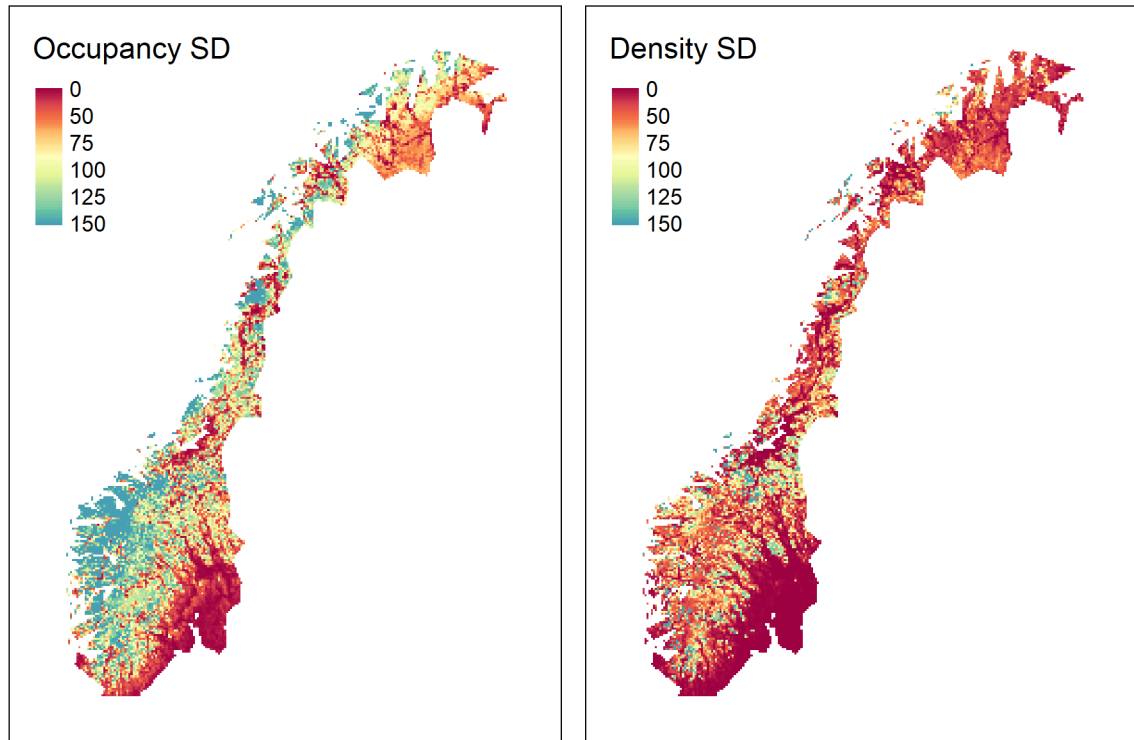
376

377 Uncertainty analysis

378 Uncertainty in the grid-level occupancy estimates had larger effects on the uncertainty of the  
 379 national abundance estimate than uncertainty in the grid-level abundance estimates (median  
 380 SD caused by each: 32 vs 81) (Fig. 6). Uncertainty in the grid-level occupancy estimates was  
 381 most influential along the western coast of central and southern Norway (Fig. 6). Uncertainty  
 382 in the abundance estimates had the greatest effect within the core alpine areas where the  
 383 density of ptarmigan is the highest. The lowest uncertainty for both data types was in the  
 384 forested areas of southeast Norway, explained by the expected low abundance and occupancy.  
 385 Grids with high uncertainty in both occupancy and abundance were found in central Norway.

386

387



388

389 Fig. 6 The impact of grid-level uncertainty in the predictions of occupancy and abundance on  
390 the uncertainty (standard deviation of estimate) of the national population size. To facilitate  
391 comparison, the same colour scale is used for each map.

## 392 Discussion

393 The cultural shift towards open data has created new opportunities for ecologists to model  
394 species' populations, but at the same time, new challenges to develop ways to combine the  
395 different data types that are available. We show how abundance data and occurrence data can  
396 be combined to produce predictions of total population abundance for a species over a  
397 nationwide extent. Our approach takes advantage of the contrast between types of data and  
398 citizen science: coarse but spatially extensive occurrence data from opportunistic citizen  
399 science and detailed but spatially restricted abundance data from structured citizen science.  
400 We used the model to produce the first estimate of the national population size of our study  
401 species – an average of c. 1.2 million individuals of willow ptarmigan in Norway in the study  
402 period 2008-2017 – and to identify geographic regions where more data are needed to  
403 improve the national estimate.

404 Our approach combines elements of past approaches for estimating avian population  
405 sizes but in a spatially-explicit hierarchical model. Previous approaches have typically  
406 extrapolated available density estimates over the known range of a species (Thogmartin *et al.*  
407 2006; Musgrove *et al.* 2013; Stanton *et al.* 2019). Callaghan *et al.* (2021) recently produced  
408 global population size estimates for bird species based on relationships between regional  
409 abundance estimates and the number of eBird observations. Birdlife International produces  
410 global population size estimates by combining average density information with estimates of  
411 area of occupancy (<http://datazone.birdlife.org/species/spcpop>). However, these models are  
412 typically not spatially-explicit and/or do not propagate all the uncertainty in the density and  
413 occupancy estimates.

414 Recently, new approaches for data integration have been developed, combining  
415 different types of monitoring data, including presence-only, presence-absence and abundance  
416 (Miller *et al.* 2019). In so-called integrated distribution models, multiple data streams are

417 combined in the same hierarchical model that explicitly separates the observation/sampling  
418 process affecting the observed data from the true state or ecological process affecting the  
419 species (Isaac *et al.* 2020). Use of a Bayesian framework also simplifies the process of  
420 retaining all the underlying uncertainty in the different components of the model during  
421 integration. Several alternative approaches have been proposed for data integration (Pacifici *et*  
422 *al.* 2017; Miller *et al.* 2019; Simmonds *et al.* 2020), but the most commonly used method so  
423 far is based on a joint-likelihood approach, which uses different data streams to jointly infer  
424 the ecological processes, such as land-use and climate effects. The joint-likelihood approach  
425 has been most often applied to combine presence-only and presence-absence data (Simmonds  
426 *et al.* 2020), but there are also applications for combining abundance and occurrence data  
427 (Bowler *et al.* 2019; Farr *et al.* 2021). Simulation studies show that data integration in this  
428 way can increase the precision of parameter estimates, including covariate effects (Farr *et al.*  
429 2021) and temporal trends (Hertzog *et al.* 2021), by increasing the sample size of data  
430 informing the model. However, the joint-likelihood approach requires making the strong  
431 assumption about identical ecological processes generating each data type, and it remains  
432 unclear when joint-likelihood is robust to deviations from this assumption (Simmonds *et al.*  
433 2020; Suhaimi, Blair & Jarvis 2021).

434         While it has been argued on theoretical grounds that abundance and occurrence are  
435 outcomes of the same processes affecting the distribution of individuals (Kéry & Royle  
436 2016), empirical data analyses support different species dynamics for occupancy and  
437 abundance (Dennis *et al.* 2019). In our case, we allowed the models for occurrence and  
438 abundance to be independent and not to share information, justified by the large differences in  
439 spatial scale and habitats sampled by each dataset. The distance-sampling abundance survey  
440 was dedicated to the willow ptarmigan and targeted its core alpine habitats; by contrast, the  
441 occurrence datasets came from observers reporting any bird species across the range of



442 habitats available across Norway. Hence, we rather assumed that each dataset provided  
443 different information on the process affecting the species' abundance and distribution, which  
444 was supported by the estimated covariate effects – land cover variables explained variation in  
445 occupancy while climatic variables mostly explained variation in abundance at occupied sites.  
446 Further simulation studies could explore how the optimal integration approach varies with the  
447 spatial scale and coverage of each data stream.

448         Regardless of the data integration approach, population size estimates will always  
449 contain some uncertainty, which might limit the application for conservation and  
450 management. Recent studies have begun to consider how citizen scientists might be nudged to  
451 collect data in specific geographic regions to make the data more informative (Callaghan *et al.*  
452 2019). Often these regions include those with the least amount of data and hence  
453 proportionally under-sampled compared to other regions. However, the value of further data  
454 collection in a geographic region can be more complex and depend on factors such as the  
455 habitat preference and habitat breadth of the species. For the willow ptarmigan, regions with  
456 dense forest cover have low occupancy uncertainty, regardless of data availability, because it  
457 is not found in these habitats, and this can be easily modelled with the right covariates. Our  
458 analysis suggested that uncertainty in occupancy was especially high in western central and  
459 southern Norway, where habitat might be suitable but there are less data. Hence, targeted data  
460 collection in these areas may be most beneficial. However, as a caveat, this analysis did not  
461 consider other causes of uncertainty, including model structure, which also might be further  
462 investigated, but we used a typical range of habitat and climate covariates.

463         We applied our method to the willow ptarmigan in Norway, which currently has the  
464 IUCN status of “least concern”, but like similar montane species, has been declining across  
465 Fennoscandia (Lehikoinen *et al.* 2019), although this was not evident during the recent time-  
466 frame of our study. Hence, knowledge of its population size could be important for future red

467 list decisions. As this species interacts with a range of other species in alpine regions - as both  
468 a herbivore and as prey, its absolute abundance also has implications for other species in the  
469 food web (Bowler *et al.* 2020). Moreover, the ptarmigan is a game species and information on  
470 population size is one of the factors determining harvesting quotas (Eriksen, Moa & Nilsen  
471 2018).

472         Methods for data integration arrive at a time when ecologists have increasing access to  
473 diverse open datasets on species' occurrences and abundances. Since different datasets come  
474 with different strengths and weaknesses, stronger inferences can often be made by combining  
475 multiple sources rather than focusing on a single data source. Because of the rarity of large-  
476 scale abundance data, the value of absolute population size estimates is increasingly  
477 overlooked in ecological research. Hence, data integration is particular exciting for studies of  
478 the abundance dynamics of species. Currently data integration is rather used retrospectively,  
479 for analysis of available data, but as the tools become commonplace, data integration might be  
480 planned already in the design stages of monitoring schemes to maximize the complementarity  
481 of different datasets and expected benefits of integration.

482

483

484

485

486

487

488

489

490

491

492 **Author contributions**

493 DB led the project, in discussion with EN. DB performed the analysis and wrote the first  
494 draft. EN revised and edited the paper.

495

496 **Acknowledgements**

497 The authors declare no conflicts of interest. The study was supported by the Research Council  
498 of Norway (grant no. 251112) and by base funding from the Norwegian Institute for Nature  
499 Research, and from the Environment Agency of Norway supporting the line-transect survey.  
500 DB also appreciates the support of the German Research Foundation (DFG) for funding the  
501 sMon working group (Trend analysis of biodiversity data in Germany) through the iDiv (DFG  
502 FZT 118, 202548816).

503

504 **Data availability**

505 All data (species and environmental) used in the analysis will be archived in the Dryad  
506 database. Updated data for the line-transect survey are also available via GBIF (Nilsen E B,  
507 Vang R & E 2021; Nilsen E B *et al.* 2021; Nilsen E.B., Vang R. & J.I. 2021). Code for the  
508 analysis are available at: <https://github.com/bowlerbear/ptarmiganUpscaling> and will be  
509 archived at Zenodo on acceptance.

510

511

512

513

514

515

516 References

- 517 Blumenrath, S. & Hanssen, F. (2010) Beregning av areal. *Datagrunnlag for Naturindeks 2010* (ed. S.  
518 Nybø), pp. 8-29.
- 519 Botsch, Y., Jenni, L. & Kery, M. (2020) Field evaluation of abundance estimates under binomial and  
520 multinomial N-mixture models. *Ibis*, **162**, 902-910.
- 521 Bowler, D.E., Kvasnes, M.A.J., Pedersen, H.C., Sandercock, B.K. & Nilsen, E.B. (2020) Impacts of  
522 predator-mediated interactions along a climatic gradient on the population dynamics of an  
523 alpine bird. *Proceedings of the Royal Society B-Biological Sciences*, **287**.
- 524 Bowler, D.E., Nilsen, E.B., Bischof, R., O'Hara, R.B., Yu, T.T., Oo, T., Aung, M. & Linnell, J.D.C. (2019)  
525 Integrating data from different survey types for population monitoring of an endangered  
526 species: the case of the Eld's deer. *Scientific Reports*, **9**.
- 527 Broms, K.M., Hooten, M.B. & Fitzpatrick, R.M. (2016) Model selection and assessment for multi-  
528 species occupancy models. *Ecology*, **97**, 1759-1770.
- 529 Buckland, S.T., Anderson, D.R., Burnham, K.P., Laake, J.L., Borchers, D.L. & Thomas, L. (2001)  
530 *Introduction to distance sampling: estimating abundance of biological populations*. Oxford  
531 University Press, London.
- 532 Buckland, S.T. & Johnston, A. (2017) Monitoring the biodiversity of regions: Key principles and  
533 possible pitfalls. *Biological Conservation*, **214**, 23-34.
- 534 Callaghan, C.T., Poore, A.G.B., Major, R.E., Rowley, J.J.L. & Cornwell, W.K. (2019) Optimizing future  
535 biodiversity sampling by citizen scientists. *Proceedings of the Royal Society B-Biological  
536 Sciences*, **286**.
- 537 Collen, B., Loh, J., Whitmee, S., McRae, L., Amin, R. & Baillie, J.E.M. (2009) Monitoring Change in  
538 Vertebrate Abundance: the Living Planet Index. *Conservation Biology*, **23**, 317-327.
- 539 Dennis, E.B., Brereton, T.M., Morgan, B.J.T., Fox, R., Shortall, C.R., Prescott, T. & Foster, S. (2019)  
540 Trends and indicators for quantifying moth abundance and occupancy in Scotland. *Journal of  
541 Insect Conservation*, **23**, 369-380.
- 542 Dornelas, M., Gotelli, N.J., Shimadzu, H., Moyes, F., Magurran, A.E. & McGill, B.J. (2019) A balance of  
543 winners and losers in the Anthropocene. *Ecology Letters*, **22**, 847-854.
- 544 Eriksen, L.F., Moa, P.F. & Nilsen, E.B. (2018) Quantifying risk of overharvest when implementation is  
545 uncertain. *Journal of Applied Ecology*, **55**, 482-493.
- 546 Farr, M.T., Green, D.S., Holekamp, K.E. & Zipkin, E.F. (2021) Integrating distance sampling and  
547 presence-only data to estimate species abundance. *Ecology*, **102**.
- 548 Hertzog, L.R., Frank, C., Klimek, S., Roder, N., Bohner, H.G.S. & Kamp, J. (2021) Model-based  
549 integration of citizen science data from disparate sources increases the precision of bird  
550 population trends. *Diversity and Distributions*, **27**, 1106-1119.
- 551 Hewson, C.M., Miller, M., Johnston, A., Conway, G.J., Saunders, R., Marchant, J.H. & Fuller, R.J. (2018)  
552 Estimating national population sizes: Methodological challenges and applications illustrated  
553 in the common nightingale, a declining songbird in the UK. *Journal of Applied Ecology*, **55**,  
554 2008-2018.
- 555 Isaac, N.J.B., Jarzyna, M.A., Keil, P., Dambly, L.I., Boersch-Supan, P.H., Browning, E., Freeman, S.N.,  
556 Golding, N., Guillera-Aroita, G., Henrys, P.A., Jarvis, S., Lahoz-Monfort, J., Pagel, J., Pescott,  
557 O.L., Schmucki, R., Simmonds, E.G. & O'Hara, R.B. (2020) Data Integration for Large-Scale  
558 Models of Species Distributions. *Trends in Ecology & Evolution*, **35**, 56-67.
- 559 Isaac, N.J.B., van Strien, A.J., August, T.A., de Zeeuw, M.P. & Roy, D.B. (2014) Statistics for citizen  
560 science: extracting signals of change from noisy ecological data. *Methods in Ecology and  
561 Evolution*, **5**, 1052-1060.
- 562 IUCN (2012) IUCN Red List Categories and Criteria: Version 3.1. Second edition. pp. 32. IUCN, Gland,  
563 Switzerland and Cambridge, UK.
- 564 Johnson, D.H. (2008) In Defense of indices: The case of bird surveys. *Journal of Wildlife Management*,  
565 **72**, 857-868.

566 Jones, J.P.G. (2011) Monitoring species abundance and distribution at the landscape scale. *Journal of*  
567 *Applied Ecology*, **48**, 9-13.

568 Kery, M., Gardner, B. & Monnerat, C. (2010) Predicting species distributions from checklist data using  
569 site-occupancy models. *Journal of Biogeography*, **37**, 1851-1862.

570 Kéry, M. & Royle, J.A. (2016) *Applied hierarchical modeling in ecology: Volume 1*. Academic Press.

571 Kolecek, J., Schleuning, M., Burfield, I.J., Baldi, A., Bohning-Gaese, K., Devictor, V., Fernandez-Garcia,  
572 J.M., Horak, D., Van Turnhout, C.A.M., Hnatyna, O. & Reif, J. (2014) Birds protected by  
573 national legislation show improved population trends in Eastern Europe. *Biological*  
574 *Conservation*, **172**, 109-116.

575 Kunin, W.E. (1998) Extrapolating species abundance across spatial scales. *Science*, **281**, 1513-1515.

576 Kvasnes, M.A.J., Pedersen, H.C. & Nilsen, E.B. (2018) Quantifying suitable late summer brood habitats  
577 for willow ptarmigan in Norway. *Bmc Ecology*, **18**.

578 Lehikoinen, A., Brotons, L., Calladine, J., Campedelli, T., Escandell, V., Flousek, J., Grueneberg, C.,  
579 Haas, F., Harris, S., Herrando, S., Husby, M., Jiguet, F., Kalas, J.A., Lindstrom, A., Lorrilliere, R.,  
580 Molina, B., Pladevall, C., Calvi, G., Sattler, T., Schmid, H., Sirkia, P.M., Teufelbauer, N. &  
581 Trautmann, S. (2019) Declining population trends of European mountain birds. *Global*  
582 *Change Biology*, **25**, 577-588.

583 McCrea, R.S. & Morgan, B.J. (2014) *Analysis of capture-recapture data*. CRC press.

584 McGill, B. & Collins, C. (2003) A unified theory for macroecology based on spatial patterns of  
585 abundance. *Evolutionary Ecology Research*, **5**, 469-492.

586 Metz, M., Rocchini, D. & Neteler, M. (2014) Surface Temperatures at the Continental Scale: Tracking  
587 Changes with Remote Sensing at Unprecedented Detail. *Remote Sensing*, **6**, 3822-3840.

588 Miller, D.A.W., Pacifici, K., Sanderlin, J.S. & Reich, B.J. (2019) The recent past and promising future for  
589 data integration methods to estimate species' distributions. *Methods in Ecology and*  
590 *Evolution*, **10**, 22-37.

591 Musgrove, A., Aebischer, N., Eaton, M., Hearn, R., Newson, S., Noble, D., Parsons, M., Risely, K. &  
592 Stroud, D. (2013) Population estimates of the birds in Great Britain and the United Kingdom.  
593 *British Birds*, **106**, 64-100.

594 Nilsen E B, Vang R & E, A. (2021) Tetraonid line transect surveys from Norway: Data from  
595 Finnmarkseiendommen (FeFo). Version 1.6. Norwegian Institute for Nature Research.  
596 Sampling event dataset <https://doi.org/10.15468/s7c8qd>. Accessed via GBIF.org.

597 Nilsen E B, Vang R, Kjønnsberg M & J, K.M.A. (2021) Tetraonid line transect surveys from Norway: Data  
598 from Fjellstyrene. Version 1.6. Norwegian Institute for Nature Research. Sampling event  
599 dataset <https://doi.org/10.15468/975ski>. Accessed via GBIF.org.

600 Nilsen E.B., Vang R. & J.I., B. (2021) Tetraonid line transect surveys from Norway: Data from Statskog.  
601 Version 1.7. Norwegian Institute for Nature Research. Sampling event dataset  
602 <https://doi.org/10.15468/q2ehlk>. Accessed via GBIF.org.

603 Nilsen, E.B., Vang, R., Kjønnsberg, M. & Kvasnes, M.A.J. (2020) Tetraonid line transect surveys from  
604 Norway: Data from Fjellstyrene. Version 1.3. Norwegian Institute for Nature Research.  
605 Sampling event dataset <https://doi.org/10.15468/975ski>.

606 Outhwaite, C.L., Gregory, R.D., Chandler, R.E., Collen, B. & Isaac, N.J.B. (2020) Complex long-term  
607 biodiversity change among invertebrates, bryophytes and lichens. *Nature Ecology &*  
608 *Evolution*, **4**, 384+.

609 Pacifici, K., Reich, B.J., Miller, D.A.W., Gardner, B., Stauffer, G., Singh, S., McKerrow, A. & Collazo, J.A.  
610 (2017) Integrating multiple data sources in species distribution modeling: a framework for  
611 data fusion. *Ecology*, **98**, 840-850.

612 Pagel, J., Anderson, B.J., O'Hara, R.B., Cramer, W., Fox, R., Jeltsch, F., Roy, D.B., Thomas, C.D. &  
613 Schurr, F.M. (2014) Quantifying range-wide variation in population trends from local  
614 abundance surveys and widespread opportunistic occurrence records. *Methods in Ecology*  
615 *and Evolution*, **5**, 751-760.

- 616 Pollock, K.H., Nichols, J.D., Simons, T.R., Farnsworth, G.L., Bailey, L.L. & Sauer, J.R. (2002) Large scale  
617 wildlife monitoring studies: statistical methods for design and analysis. *Environmetrics*, **13**,  
618 105-119.
- 619 Reed, D.H., O'Grady, J.J., Brook, B.W., Ballou, J.D. & Frankham, R. (2003) Estimates of minimum  
620 viable population sizes for vertebrates and factors influencing those estimates. *Biological*  
621 *Conservation*, **113**, 23-34.
- 622 Simmonds, E.G., Jarvis, S.G., Henrys, P.A., Isaac, N.J.B. & O'Hara, R.B. (2020) Is more data always  
623 better? A simulation study of benefits and limitations of integrated distribution models.  
624 *Ecography*, **43**, 1413-1422.
- 625 Soroye, P., Ahmed, N. & Kerr, J.T. (2018) Opportunistic citizen science data transform understanding  
626 of species distributions, phenology, and diversity gradients for global change research. *Global*  
627 *change biology*.
- 628 Stanton, J.C., Blancher, P., Rosenberg, K.V., Panjabi, A.O. & Thogmartin, W.E. (2019) Estimating  
629 uncertainty of North American landbird population sizes. *Avian Conservation and Ecology*,  
630 **14**.
- 631 Suhaimi, S.S.A., Blair, G.S. & Jarvis, S.G. (2021) Integrated species distribution models: A comparison  
632 of approaches under different data quality scenarios. *Diversity and Distributions*, **27**, 1066-  
633 1075.
- 634 Thogmartin, W.E., Howe, F.P., James, F.C., Johnson, D.H., Reed, E.T., Sauer, J.R. & Thompson, F.R.  
635 (2006) A review of the population estimation approach of the North American landbird  
636 conservation plan. *Auk*, **123**, 892-904.
- 637 Tobler, M.W., Hartley, A.Z., Carrillo-Percegué, S.E. & Powell, G.V.N. (2015) Spatiotemporal  
638 hierarchical modelling of species richness and occupancy using camera trap data. *Journal of*  
639 *Applied Ecology*, **52**, 413-421.
- 640 Van Strien, A.J., Pannekoek, J. & Gibbons, D.W. (2001) Indexing European bird population trends  
641 using results of national monitoring schemes: a trial of a new method. *Bird Study*, **48**, 200-  
642 213.
- 643 van Strien, A.J., van Swaay, C.A.M. & Termaat, T. (2013) Opportunistic citizen science data of animal  
644 species produce reliable estimates of distribution trends if analysed with occupancy models.  
645 *Journal of Applied Ecology*, **50**, 1450-1458.
- 646 Yoccoz, N.G., Nichols, J.D. & Boulinier, T. (2001) Monitoring of biological diversity in space and time.  
647 *Trends in Ecology & Evolution*, **16**, 446-453.
- 648 Zipkin, E.F., Grant, E.H.C. & Fagan, W.F. (2012) Evaluating the predictive abilities of community  
649 occupancy models using AUC while accounting for imperfect detection. *Ecological*  
650 *Applications*, **22**, 1962-1972.

651